Structures 59 (2024) 105810

Contents lists available at ScienceDirect

Structures

journal homepage: www.elsevier.com/locate/structures

Characterization of the elevated temperature behaviour of demountable shear connectors in steel-concrete composite beams through push-out tests

R. Mansilla [a], A. Espinós [a], C. Odenbreit [b], I. Payá-Zaforteza [a], M.L. Romero [a,*]

[a] ICITECH, Universitat Politècnica de València, Valencia, Spain
[b] Faculty of Science Technology and Medicine, University of Luxembourg, Luxembourg

ARTICLE INFO

Keywords:
Reusable systems
Push-out tests
Circular economy
Fire resistance
Shear connectors

ABSTRACT

Demountable shear connectors are a key component of reusable structural systems. The intention behind the development of these systems is substituting, or at least providing a valid alternative to the widely utilized beam-to-slab connection via shear studs, which are welded to the flange of the steel profile and embedded in the concrete slab, therefore eliminating the possibility for the slabs to be reused in a new structure. To ensure that these demountable connectors are a valid option in practice, it is necessary to analyse them under different actions, including the fire situation. This is the primary purpose of the experimental campaign presented in this investigation, where a series of push-out tests at elevated temperatures are performed to extend the previously available results at ambient temperature, as a response for the need of characterization of the behaviour of the proposed demountable shear connectors in the fire situation, thus facilitating their applicability in the construction sector. This study shows how temperature affects the shear resistance of the connectors, their ductility, and the slip resistance. The available design provisions in EN 1993–1-8 and the reduction factors in Annex D of EN 1993–1-2 for bolts loaded in shear are tentatively applied to high temperatures, as a way to assess their validity for fire design.

1. Introduction

The demand for sustainable building solutions that minimize the associated carbon footprint is increasing in recent times. One of the main concerns related to traditional building systems is their lack of reusability, turning most of their components into waste once the structure is demolished and presenting high greenhouse gas emissions during the phases of their life cycle. A big goal for the construction industry, considering how much of an impact it generates on the environment, is to move from a linear economy model to a circular economy model, where the lifecycle of materials is extended and the reusability of the structural components is an inherent feature of the building.

The first investigations on demountable bolted shear connectors were conducted by Dallam [1] and Marshall et al. [2] almost five decades ago. However, the research on demountable shear connections is still very limited compared to welded studs in the past decades. Dedic and Klaiber [3], Sedlacek et al. [4], Pavlović [5,6], Dai et al. [7], Rehman et al. [8] and Wang et al. [9] investigated encased studs or bolts that were placed in pre-drilled holes of the steel flange before concrete casting. Kwon et al. [10] studied the strengthening possibilities of existing non-composite steel girder bridges with post-installed shear connectors.

Through bolts that were used in combination with prefabricated deck elements were investigated by Chen et al. [11] and Lee and Bradford [12]. More recently, Suwaed and Karavasilis [13] developed a demountable shear connection with through bolts, where the bolt clearance was grouted after installation. Feidaki and Vasdravellis [14] conducted push-out tests on demountable shear connectors that used a steel-yielding mechanism provided by a steel section with slotted holes. Blind bolts were investigated by Ban et al. [15], Pathirana et al. [16] and Uy et al. [17].

Although the previously studied solutions facilitate the demounting process, they provide different levels of reusability. For example, the embedded bolts and studs are not replaceable. When dismantled, they stand out of the concrete. This makes the threads vulnerable during transportation. If thread damage occurs, the reuse potential of the slab element is lost. On the other hand, in the case of through bolts, it is sufficient to replace the bolts to maintain the reusability of the slab and thus lengthen the service life of the system.

The project REDUCE [18], carried out at the University of

* Corresponding author.
E-mail address: mromero@mes.upv.es (M.L. Romero).

https://doi.org/10.1016/j.istruc.2023.105810
Received 20 July 2023; Received in revised form 2 December 2023; Accepted 21 December 2023
Available online 2 January 2024

Luxembourg and funded by the "Research Fund for Coal and Steel" of the European Commission, examined two types of demountable shear connection solutions to develop reusable and modularized flooring systems for concrete floor slabs with down-stand beams. The outcomes of the referred project, supported by the PhD dissertation from Kozma [19], demonstrated the functionality and reuse capacity of the proposed connection systems. The first system was the so-called 'Cylinder System', denoted as 'P3.1′ (Fig. 1a). The second one was named 'Coupler System', designated as 'P15.1′ (Fig. 1b).

Even though these systems were mechanically analysed by performing push-out tests at ambient temperature [20], they have not been tested under the combined action of mechanical load and elevated temperatures simultaneously. That is the starting point of the research project FIREDUCE, which is currently underway at ICITECH, Universitat Politècnica de València, Spain – the first outcomes being presented in this paper –. This project aims to provide results that allow for a precise understanding of the behaviour and failure mechanism of these systems in a fire situation. The same types of demountable shear connectors as those previously studied at the University of Luxembourg [18] are studied in this new project, with the focus on their fire behaviour, an aspect that has not been addressed yet, being much needed for fully characterizing these types of connectors before their introduction into the market.

It is worth mentioning that, although studies on the fire behaviour of demountable shear connectors have not been carried out to date, the effect of temperature was previously studied for the more common system of welded shear studs. Yasuda et al. [21] performed an experimental study on the shear strength of shear studs at elevated temperatures for composite beams, considering different types of slabs (reinforced concrete slab and concrete slab with profiled steel deck). Chen et al. [22] studied the performance of shear connectors in composite beams at high temperature, utilizing slabs with profiled sheeting, also performing a complementary numerical analysis and a parametric study.

As it is the case with any other structural systems, providing a framework that establishes the performance in case of fire of the proposed demountable solutions for the future development of practical design recommendations that guarantee the accomplishment of the safety regulations is a concern that must be addressed.

To give more insight into this question, this paper presents the results of an experimental campaign of elevated temperature push-out tests on the proposed type of demountable shear connectors.

2. Experimental campaign

2.1. Preparation of specimens

The experimental campaign presented in this work is focused on analyzing the behaviour at elevated temperatures of the demountable shear connectors introduced in the previous section, by combining the standard push-out tests protocol with the heating of the test specimens to certain target temperatures. This section provides a detailed description of each connection system tested.

The dimensions of the different components used at each of the connection systems replicated those previously studied at the University of Luxembourg [18], as the aim of the present investigation is to extend the characterization of the proposed demountable connection systems to elevated temperatures.

The first system is known as 'Cylinder system', also denoted as 'P3.1′, whose main feature is a steel cylinder with a through bolt, see Fig. 1a). The components of this system are the following: an HEB 260 profile with S355 steel grade, an L 75 × 75 × 5 mm S355 steel profile, a steel tube CHS 33.7 × 4 × 90 mm S355 for materializing the cylinder, pretensioned M20 through bolts with a grade 8.8, steel washer plates 37 × 2 mm, hexagonal nuts with a thickness of 15 mm and an S355 steel plate on top of the cylinder with dimensions 85 × 85 × 5 mm. The system is connected to two portions of a reinforced concrete slab.

The second system is known as the "Coupler system", also referred to as 'P15.1′, see Fig. 1b). The system is composed by a coupler, with a steel grade 10.9, welded to an L 75 × 75 × 5 mm S355 steel profile. Two M20 grade 8.8 bolts are connected to the coupler. Both the upper bolt and coupler remain embedded in the concrete. The lower bolt is the one responsible for materializing the demountable connection between the concrete slab and the HEB 260 beam. The washer plates and the nuts utilized in this system are the same as those utilized for the P3.1 system. The purpose of using a coupler with a higher steel grade than the one being used for the bolts is to force the connection to fail because of the failure of the replaceable element of the system, which is the lower bolt, instead of by failure of any part that belongs to the slab, which would lead to the loss of its reusability. Both systems share this design concept.

The specimens for the push-out tests consisted of an HEB 260 steel profile of 900 mm length to which four solid concrete slab portions of

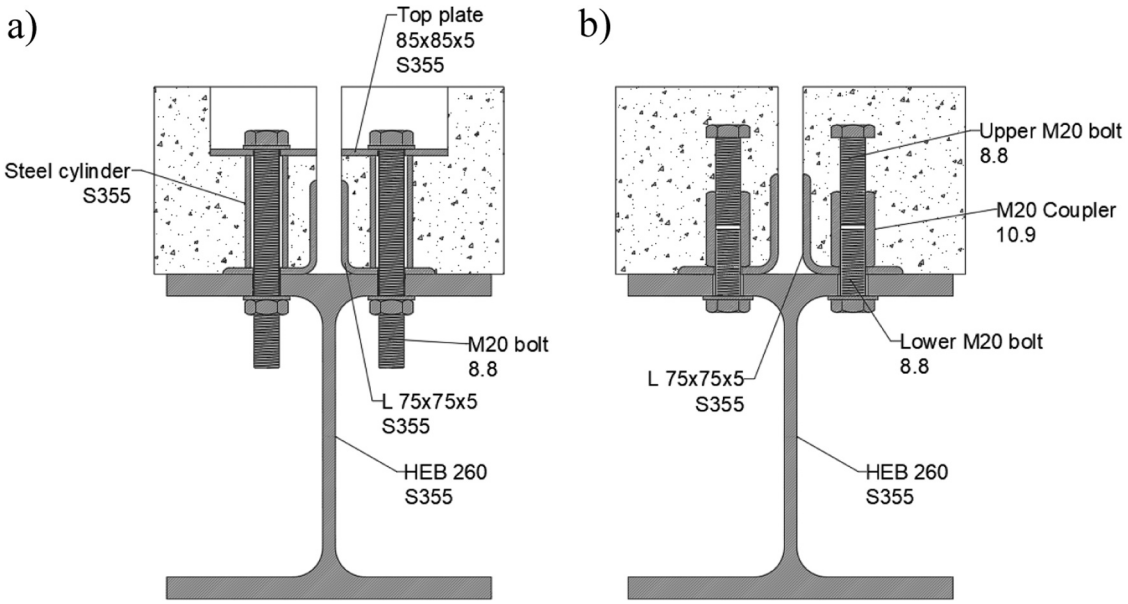

Fig. 1. a) 'Cylinder system' (P3.1) and b) 'Coupler system' (P15.1) configurations.

150 mm depth were attached through the described demountable connectors, see Fig. 2a). A test specimen ready for being inserted into the testing rig is shown in Fig. 2b).

The length of the concrete slab portions was the same of the HEB profile (900 mm), but the slab portions were attached to the steel profile flanges with a vertical offset of 65 cm, so that the load could be applied only to the top end of the steel profile. The push-out tests configuration was double-mounted, in a way that the connection between the steel profile and the concrete slabs was materialized on each flange (two bolts per flange). Also, two levels of connectors were disposed along the length of the specimen, with a distance of 333 mm between them. In total, eight connectors were used on each test.

The portions of reinforced concrete slabs connected to the HEB profile are common to both systems. The reinforcement of the concrete slabs consists of two layers of ribbed bars of ø8 mm grade B 500 S, see Fig. 3.

A custom formwork was used for the fabrication of the concrete slabs, see Fig. 4a). This formwork allowed for the concrete pouring of 16 reinforced concrete slab portions simultaneously, which could be used to generate four push-out test specimens at once. Some details of the slab reinforcement for the cylinder system are shown in Fig. 4b).

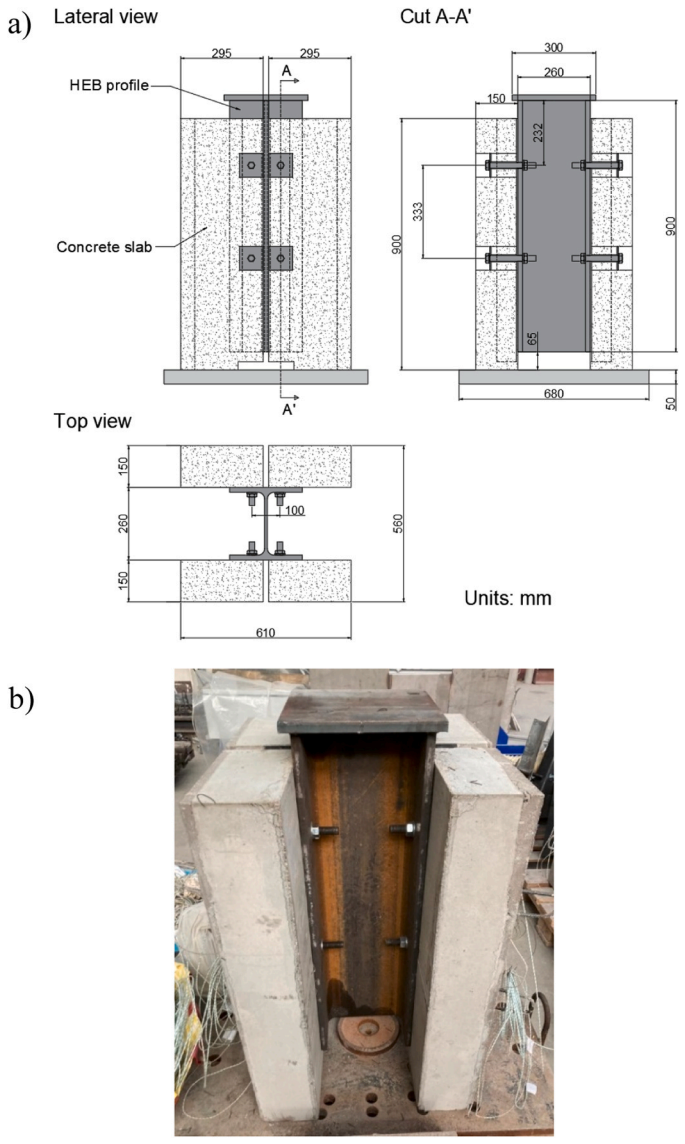

Fig. 2. Push-out test specimens: a) schematic views and annotated dimensions; b) specimen ready for testing.

2.2. Material tests

Coupon tests were performed for all the steel components of the connection system (HEB profile, L-profile and bolts) to obtain the real yield strength and ultimate tensile strength values. The results of these material tests are given in Table 1. Regarding the concrete of the slabs, cube specimens with dimensions 150 × 150 × 150 mm were subjected to compression tests. The mean value of the compressive cube strength for the concrete mix prepared for each system is also presented in Table 1.

A dynamometric torque wrench was used to apply the desired pretension force to the bolts. An isolated test materialized with the connector and a load cell attached to it was performed to calibrate the tool for each of the connection systems. Fig. 5 shows the setup of the isolated pretension test, while Table 2 provides the values of the applied torque and the effective pretension force measured by the load cell.

A comparison between the theoretical values of the pretension force and those obtained experimentally from the isolated pretension tests was made. Eq. (1) provides the expression for the calculation of the pretension force of the bolts N_0, which is adapted from Clause 3.6.1(2) in EN 1993–1-8 [23], to be used with the measured ultimate tensile strength (f_{ub} = 858 MPa for the 8.8 bolt, as given in Table 1), being A_s the area of the bolt, equal to 245 mm^2.

$$N_0 = 0,7 \cdot f_{ub} \cdot A_s \tag{1}$$

The torque corresponding to N_0 is denoted as M_t, and it can be obtained by means of Eq. (2). Parameter d is the diameter of the bolt, which is equal to 20 mm for M20 bolts.

$$M_t = 0,18 \cdot d \cdot N_0 \tag{2}$$

The theoretical values of the pretension force arising from the presented equations are 137 kN for P3.1 system and 172 kN for P15.1 system. As can be seen, the difference of the measured values with respect to the theoretical values was residual, guaranteeing that the required pretension force was achieved.

2.3. Specimen instrumentation and test setup

The experimental campaign presented in this work was carried out at the testing facilities of ICITECH, Universitat Politècnica de València, Spain.

Each configuration (P3.1 and P15.1) was analysed under four different levels of temperature, therefore a total of 8 tests were carried out. Three steady-state tests were carried out at different high temperature levels (300 ºC, 500 ºC and 600 ºC), plus one reference push-out test at ambient temperature (20 ºC) for each system. The reason behind the choice of these temperature thresholds is that in a real fire situation on a building, it would be highly unexpected that the connection system of the steel-concrete composite beam would reach temperatures higher than 600ºC, since it would be protected from the direct fire exposure.

The tests performed at 20 ºC are considered as reference cases, allowing for an actual understanding of the failure modes occurring in a situation where no previous damage or loss in strength was experienced by any of the components of the specimens due to temperature, retaining their full capacity.

2.3.1. Ambient temperature tests

The tests were conducted by means of a hydraulic jack with a load capacity of 5000 kN. The applied force was continuously monitored during the tests through a load cell interposed between the hydraulic jack and the top end of the specimen. A schematic view of the test setup for the ambient temperature push-out tests can be seen in Fig. 6a), together with a front view in Fig. 6b).

Four linear variable differential transducers (LVDTs) were installed for each test to obtain more precise information on the displacement evolution, one LVDT for each bolts alignment. The purpose of the LVDTs

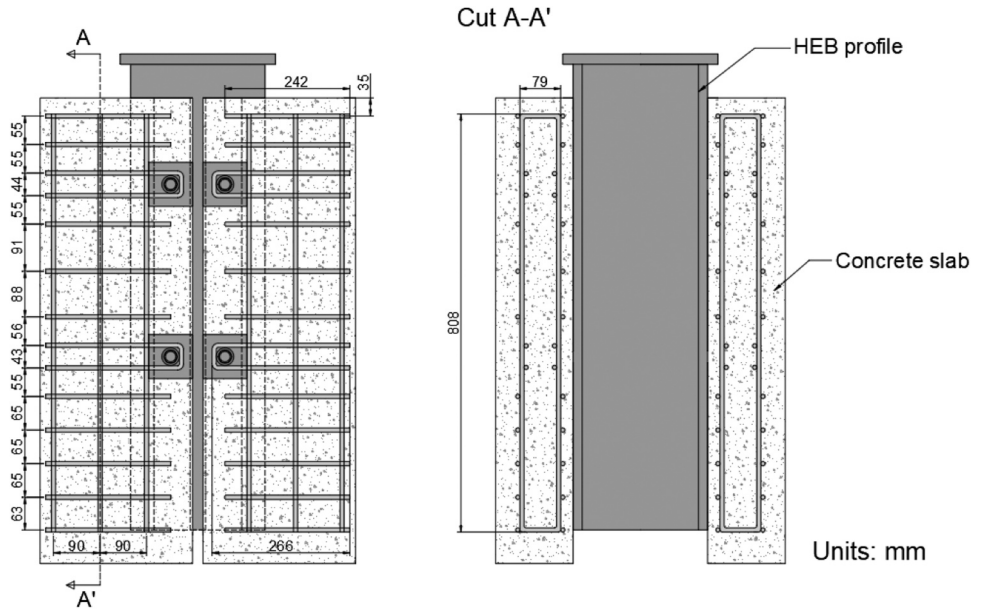

Fig. 3. Reinforcement arrangement of the concrete slabs.

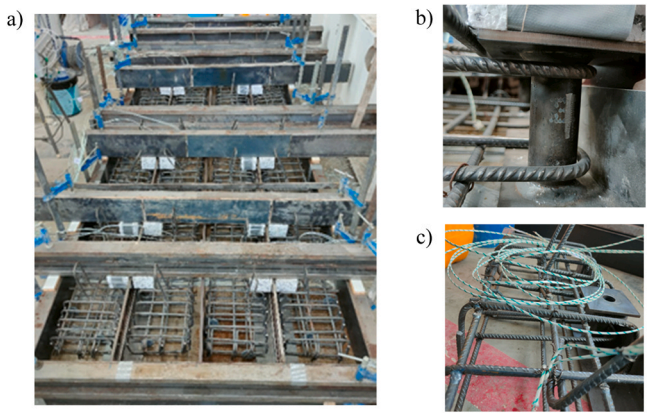

Fig. 4. Formwork (a) and details of the reinforcement (b, c) for the cylinder system before concrete pouring.

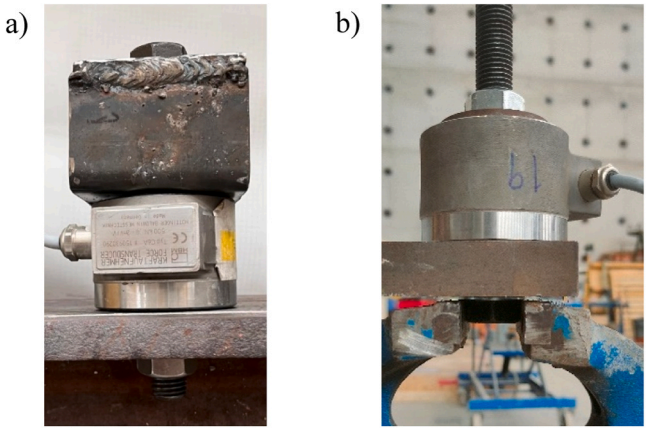

Fig. 5. Pretension test with load cell: a) cylinder system (P3.1); b) coupler system (P15.1).

Table 1
Material properties obtained from steel tensile coupon tests and concrete compression tests.

		HEB 260	L 75 × 75 × 5	M20 bolts (Grade 8.8)
Steel yield strength (f_y) (N/mm^2)	**Nominal**	355	355	640
	Measured	392,75	414	626
Steel ultimate tensile strength (f_u) (N/mm^2)	**Nominal**	510	510	800
	Measured	480,5	518	858
		P3.1	**P15.1**	
Concrete compressive cube strength (f_c) (N/mm^2)		49,49	50,66	

Table 2
Pretension tests results.

System ID	Description	Applied torque (N·m)	Applied pretension (kN)
P3.1	Cylinder system	496	142
P15.1	Coupler system	620	175

was to measure the relative vertical displacement between the steel profile and the slab elements, therefore obtaining the longitudinal slip experienced at the connection between the two, materialized by means of the rows of bolts. This measure is a required output for push-out tests by EN1994–1-1 [24]. The arrangement of LVDTs for each test specimen can be seen in Fig. 7. Note that no horizontal LVDTs were installed, as it was not possible to attach them to the inner parts of the test specimen in the elevated temperature tests due to the high temperatures reached inside the furnace chamber.

A general view corresponding to push-out test P15.1-T20 at room temperature can be seen in Fig. 8, before (a) and after failure (b).

2.3.2. *Elevated temperature tests*

The elevated temperature push-out tests were carried out at the same testing rig, equipped with a hydraulic jack of 5000 kN capacity, to which a specifically designed electric furnace was attached.

It consisted of two ad-hoc manufactured frames of rectangular shape, each one containing two ceramic heating panels of 400 × 400 mm^2 surface with inner electric resistances of 0.75 kW power each. The

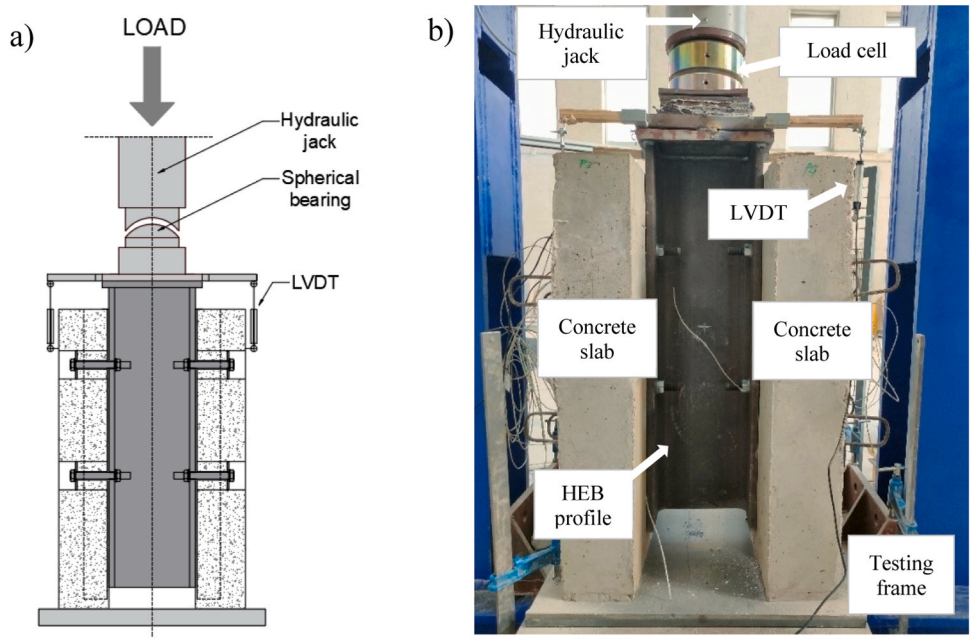

Fig. 6. Setup for the ambient temperature push-out tests: a) schematic view; b) front view.

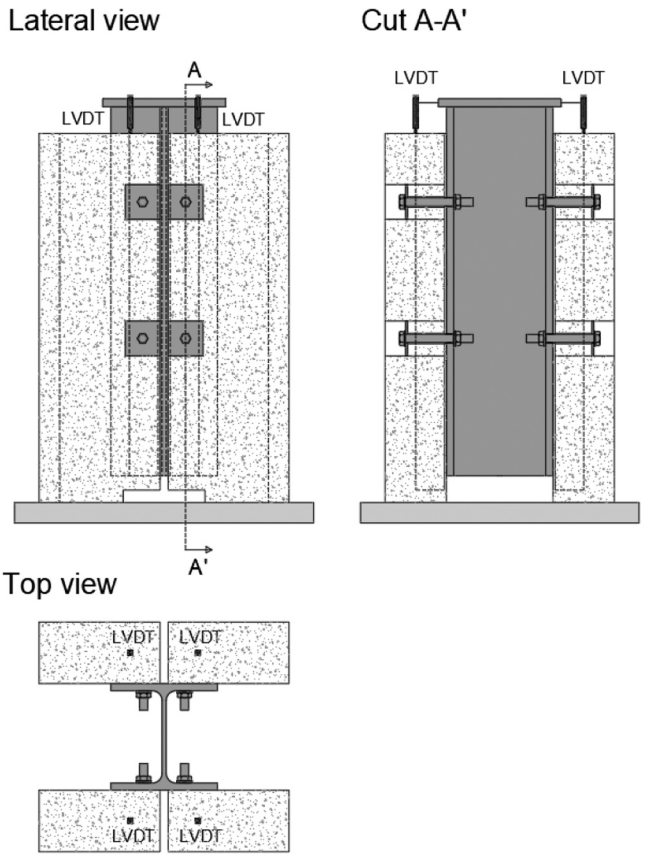

Fig. 7. LVDT arrangement.

heating panels were placed in upright position forming a closed chamber between them and the slab portions of the test specimens, using fibre blanket as insulation where required to avoid the heat loss.

A schematic view of the elevated temperature push-out test setup can be seen in Fig. 9a), together view a front view in Fig. 9b), where the heating panels attached to the testing rig can be seen. Fig. 9c) shows a

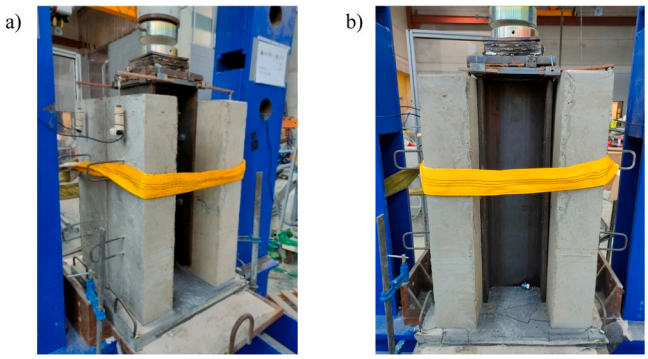

Fig. 8. Test P15.1-T20: a) specimen before test; b) specimen after failure.

detail of a heating panel assembled into the supporting frame.

The type of test performed was a thermo-mechanical steady-state test, where the specimen was heated until a target temperature was reached at a defined control point (i.e. the shear plane of the bolts). Once this target temperature was achieved, an increasing displacement was applied to the top end of the HEB profile up to failure through the hydraulic jack. The heating panels were programmed for every test performed with a target temperature at the control point equivalent to that specified for the test (300, 500, 600ºC).

The testing procedure for the thermo-mechanical tests followed the next sequence:

(1) The specimen was positioned under the hydraulic jack on a stable base that guaranteed its proper support. A high strength mortar base was fabricated for each specimen to ensure that the support base for the four concrete slabs was homogeneous. This is a requirement established by Section B.2 of EN 1994-1-1 [24] for push-out tests. A protective hood was installed between the test specimen and the load cell of the hydraulic jack to provide thermal protection for the second.
(2) The heating panels were attached to the free sides of the specimen (parallel to the web of the HEB profile) and fixed to it securely by a system of adjustable chains. This configuration allowed for a significant exposure of the demountable shear connectors to the

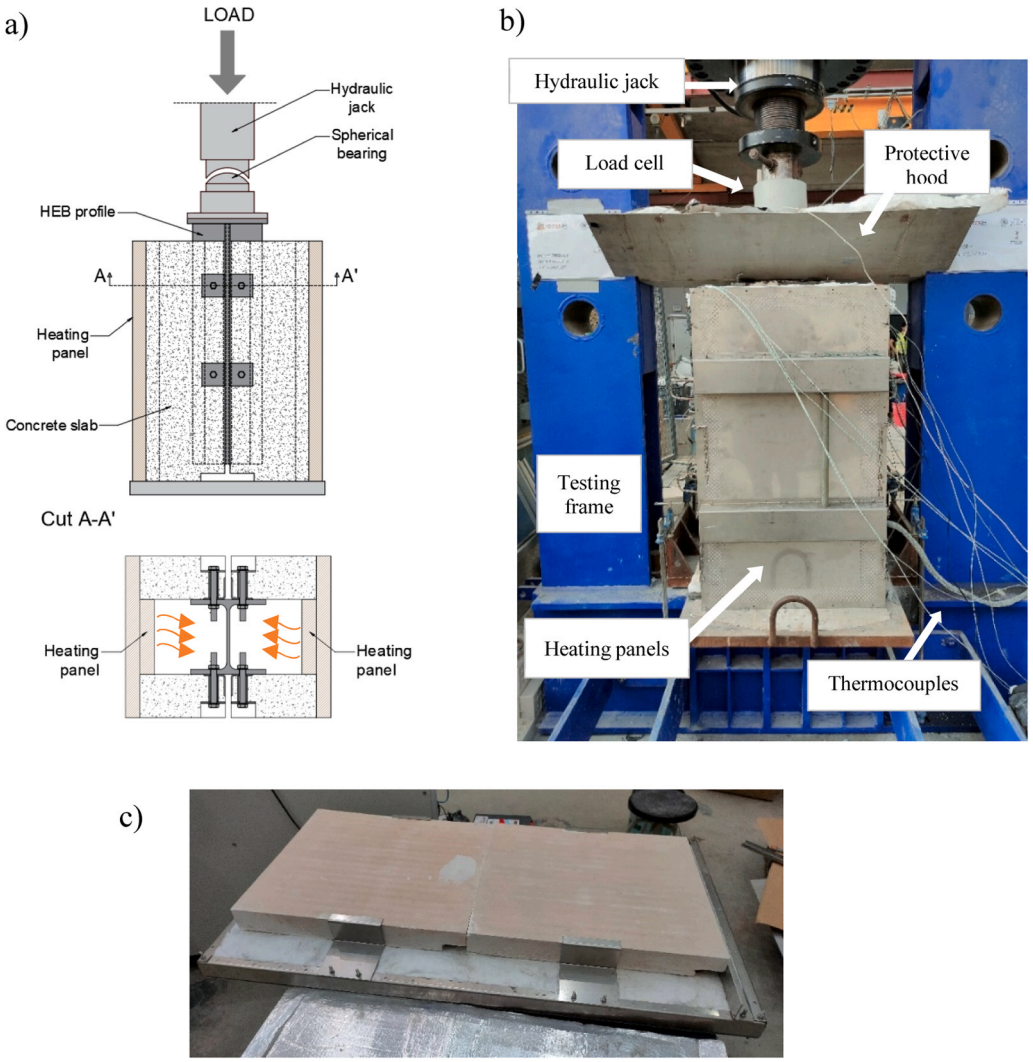

Fig. 9. Setup for the elevated temperature push-out tests: a) schematic view; b) front view; c) detail of a heating panel.

heat source. The top and bottom ends of the test specimen were covered with mineral wool to avoid temperature losses as much as possible.

(3) The heating panels were turned on and a target temperature was set up. The heating of the specimen was continued for the needed period of time so as to reach the target temperature at the established control points.

(4) Once the target temperature was reached, the loading of the specimen was started through the hydraulic jack by imposing a displacement at its top end. The applied load was increased until failure at the plane of the shear connectors occurred.

The temperature evolution at the relevant points of the tested specimens along the exposure time was measured using a set of K-type thermocouples. The total number of thermocouples utilized was dependent on the system being analysed.

The thermocouple locations were conceived in a way that allowed for adequately determining the temperature distribution of the components. For example, taking measurements at three relevant positions along the bolts (shear plane, web and outer head) provides enough information for their thermal characterization. The arrangement of thermocouples can be seen in Fig. 10.

All the thermocouples were assigned an alphanumeric code, dependent on their location. These codes are explained here, starting with system P3.1 (Fig. 10a), even though both systems share almost the same notation. Thermocouples with code 'Tbi' were utilized to measure the temperature evolution of the bolt at the shear plane, which is considered as the most relevant point of measurement. If 'Tbi' is followed by a number '1′, it means that it is located at the top bolt, while if it is followed by a '2′ it is at the lower bolt. The 'code' followed by a number rule also applies to other thermocouples. 'Tbe' was located at the exterior head of the bolt, in the contact between the top plate of the cylinder and the washer. 'BC' was used for control thermocouples located at the bolt thread right after the nut. 'Tw' was located at the weld of the cylinder or the coupler with the L-profile. The number of 'Tw' thermocouples installed was smaller than other measurement points since the installation of it was technically complicated and laborious. 'Tuf' was located at the contact between the HEB profile and the top of the concrete slab, and only one of these was installed by test. 'Tlf' is the equivalent of 'Tuf' at the bottom of the HEB profile. 'TA' was located at the middle of the web of the HEB profile, being one on each face of the profile. 'Ths' is a thermocouple located in the concrete at the level of the upper reinforcement layer, while 'Thi' is situated in the concrete at the level of the lower reinforcement layer.

System P15.1 (Fig. 10b) shares the following thermocouples in common with system P3.1: Tbi, Tw, Ths, Thi, TA, Tuf, Tlf. For this system, 'BC' was eliminated, since the process for the proper installation of the thermocouple in the head of the bolt was highly laborious. 'Tci' is specific for this system, and it is located at the contact between the thread of the bolt embedded in the concrete and the top of the coupler.

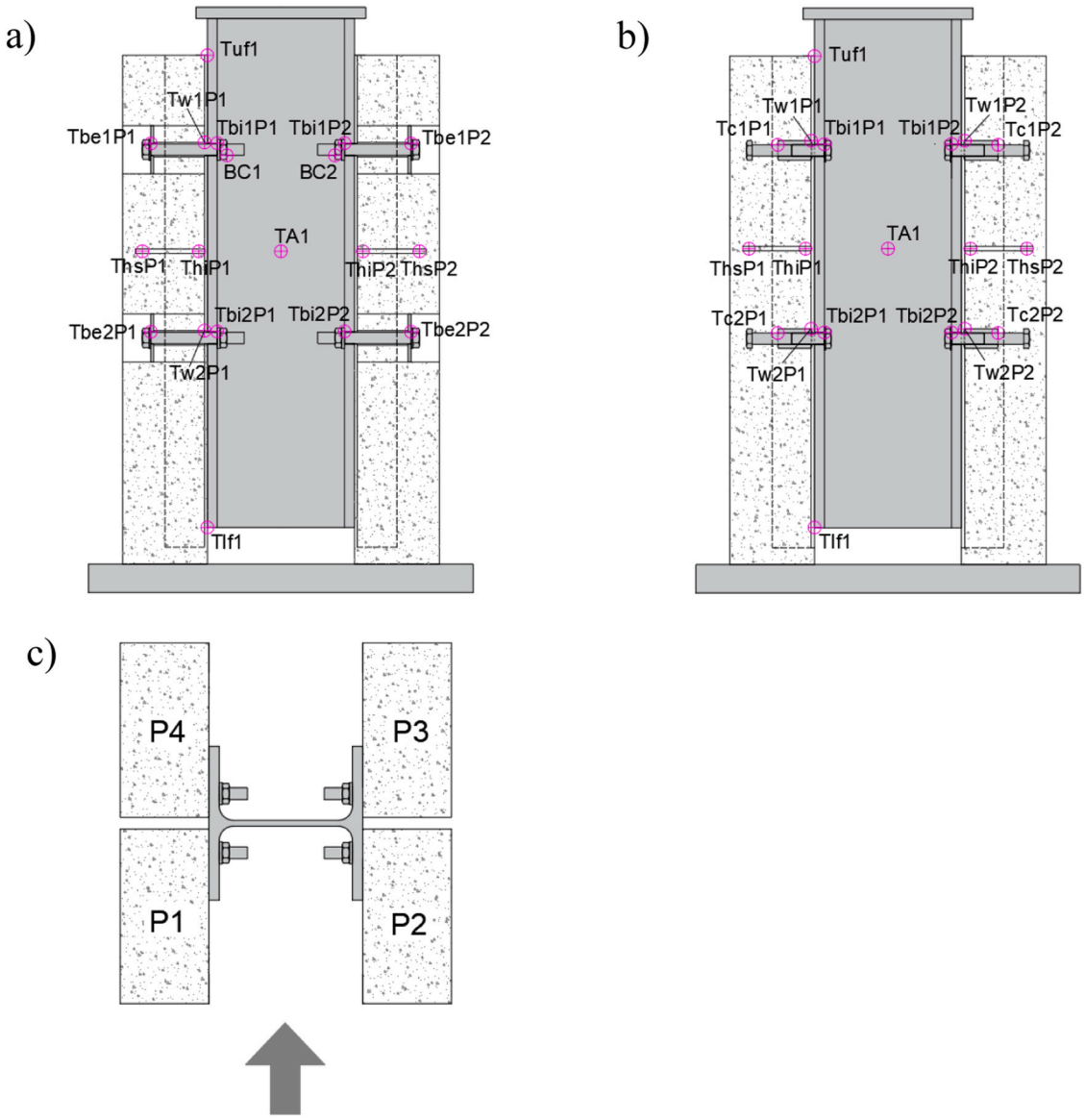

Fig. 10. Thermocouple arrangement: a) P3.1 system; b) P15.1 system; c) codification of slab elements.

The number following the letter 'P' refers to the slab element attached to the bolt (P1, P2, P3, P4), as indicated in Fig. 10c).

3. Experimental results

3.1. Failure observations at the push-out tests

The behaviour observed at the push-out tests for the demountable shear connectors studied in this experimental campaign was somewhat different from that observed in the case of headed stud connectors, where typically concrete failure precedes bolt shear failure, as reported at the DISCCO project [25]. In the investigations carried out by Pavlović [5,6] on encased bolted shear connectors, it was also observed that concrete damage always accompanied the bolt shear failure. This phenomenon was not observed, however, in the tests carried out in the present investigation, given the large bearing surface of the cast-in cylinder and of the mechanical coupler device, which prevented concrete cracking in the vicinity of the shear connectors. Therefore, it is evidenced that the L-profile, the steel cylinder and the mechanical coupler make the proposed systems robust while they help preserve the reusability of the concrete slab elements, as already proved by Kozma [19] at room temperature.

In the room temperature push-out test carried out for the cylinder system (P3.1-T20), all the bolts failed by shear, and they were easily demounted after the test. Some details of the sheared bolts are shown in Fig. 11.

However, the failure observed at the elevated temperature push-out test series for the same type of connection (cylinder system) was different. For test P3.1-T300 (300ºC target temperature), only two bolts

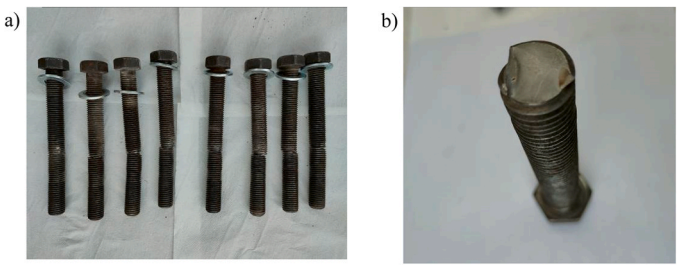

Fig. 11. Test P3.1-T20: a) bolts after shear failure; b) detail of the sheared section of one bolt.

(of the same concrete slab) experienced shear failure, which happened in a brittle way. Fig. 12a) shows the tested specimen after failure, where it can be clearly seen that the bolts in one side failed in shear, while the other two experienced a plastic deformation without reaching the shear failure, Fig. 12b). Fig. 12c) shows a detail of the section of one of the bolts which failed at the sheared plane, where it is visible how the L profile penetrated into the bolt thread.

Tests P3.1-T500 and P3.1-T600 showed a significant decrease in terms of shear capacity and failed at much lower loads as a consequence of the higher temperature thresholds reached, where the properties of the steel were severely affected. It should be mentioned that in test P3.1-T500 only one bolt of the lower row experienced shear failure, while the other bolts deformed in a ductile manner and needed to be removed with a wrench after the test was finished. During this test, the lower radiant panel of the side where the bolt failed was heating at a lower rate than the other panels, leading to a situation where two bolts were less affected by temperature, thus conserving more rigidity and absorbing more force than the other bolts. For test P3.1-T600, the complete shear failure of the bolts happened at a very late stage during the unloading phase, as the bolts behaved in a very ductile manner, which might be the reason for the large displacement observed.

In turn, for the coupler system push-out test series (P15.1), all bolts failed by shear on every test. A decrease in shear capacity and an increase of the measured maximum displacement occurred as a result of rising the target temperature, as a consequence of the material strength reduction and the increased ductility. As previously explained, the connection was designed so that the failure occurred exactly at the plane where the bolts connect the slab to the HEB profile. This is what happened on every test of this series. Fig. 13a) shows the tested specimen after failure, where it can be clearly seen that all the bolts in both sides failed in shear. A detail of two sheared bolts at different rows can be seen in Fig. 13b-c).

3.2. Temperature evolution during the heating stage

The measured temperature-time curves at the different locations where the thermocouples were installed are provided in Fig. 14.

As it can be seen in the presented graphs, thermocouples "Tbi1″ and "Tbi2″ experienced both the fastest temperature rise and the highest final temperature values reached for all tests performed, as it was expected, considering that they were installed at the inner side of the connection, with greater exposure to radiation from the heating panels.

It was also evidenced that heat convection led to higher temperatures reached at the upper row bolts (level 1) compared to those measured at the lower row bolts (level 2) in every test. Thermocouples "Tbe1″ and "Tbe2″ for the cylinder system reached much lower temperatures (with

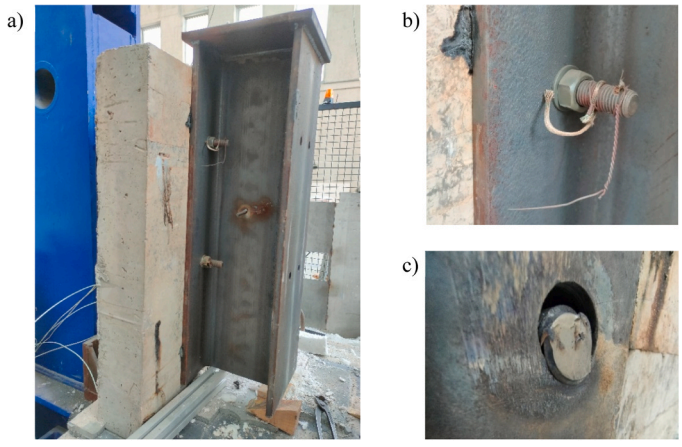

Fig. 12. Test P3.1-T300: a) specimen after failure; b) upper row deformed bolt at the no-sheared plane; c) upper row bolt after shear failure.

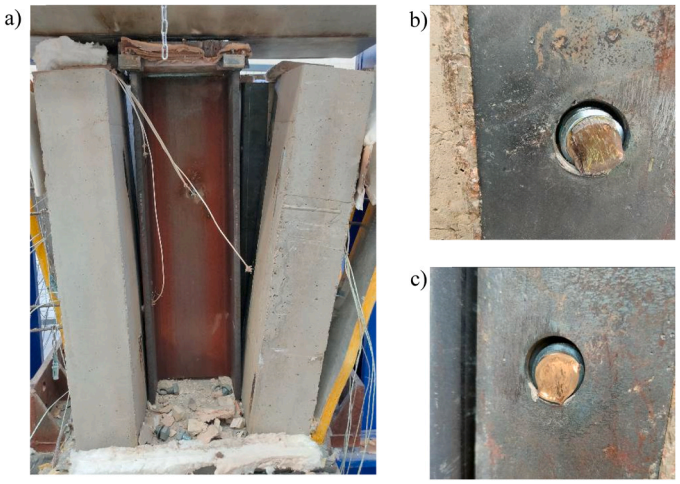

Fig. 13. Test P15.1-T300: a) specimen after failure; b) and c) details of bolts after shear failure.

temperatures about 100ºC lower at the end of the fire exposure period), as they were located at the unexposed side of the bolt (i.e. at the outer pocket). In the case of the coupler system, the lowest temperatures were found at thermocouples "Tc1″ and "Tc2″, located at the coupler, which was embedded inside the concrete mass. For the slabs, significant temperature differences were found between the measurements taken at the lower reinforcement layer (Thi) and the upper reinforcement layer (Ths), which was due to the low conductivity of concrete.

By plotting the temperature gradient along the bolt for a particular fire exposure time, as given in Fig. 15 for a selected bolt in the T500 series (located at the same position in the push-out test arrangement for both connection systems), it can be observed that, the temperatures decreased significantly along the longitudinal direction of the bolts (x-direction), from the inner thermocouple installed at the shear plane (Tbi) to that located at the outer head (Tbe) in case of the P3.1 system or at the end of the coupler for the P15.1 system, with differences greater than 100 ºC in most cases. These differences tend to increase with the fire exposure times (60, 120, 180 min), the temperature gradient being more pronounced for the cylinder system. It is important to note that the temperatures along the bolt were generally higher for the cylinder system (P3.1) than for the coupler system (P15.1), therefore it is expected that the cylinder system experiences a faster mechanical deterioration. This more favourable temperature development along the bolt at the coupler system is due to the "physical separation" along the bolt thread in this system, along with the fact that the non-exposed bolt is embedded inside the concrete mass, which due to the "heat sink" effect delays the temperature rise along the bolt. In turn, at the cylinder system, heat transfer by conduction along the bolt thread is direct from its inner (exposed) end to its outer (non-exposed) head.

The point at which the temperature was considered most relevant for every test was the one where thermocouple 'Tbi' was installed, providing the temperature for the shear plane of the bolts. Table 3 provides a summary of the temperatures registered at the shear plane of each bolt, as well as the average value, which will be used for assessing the reduction of shear capacity of the connection systems with temperature.

As some temperature differences were observed between the different bolts at each test, it was difficult to know precisely what degree of shear load each of the bolts was bearing at failure. In order to solve this, the average of the temperatures measured at the shear plane of the eight bolts at failure was used as a representative temperature for the subsequent calculations to be performed in Section 4, in order to have a uniform framework for comparison.

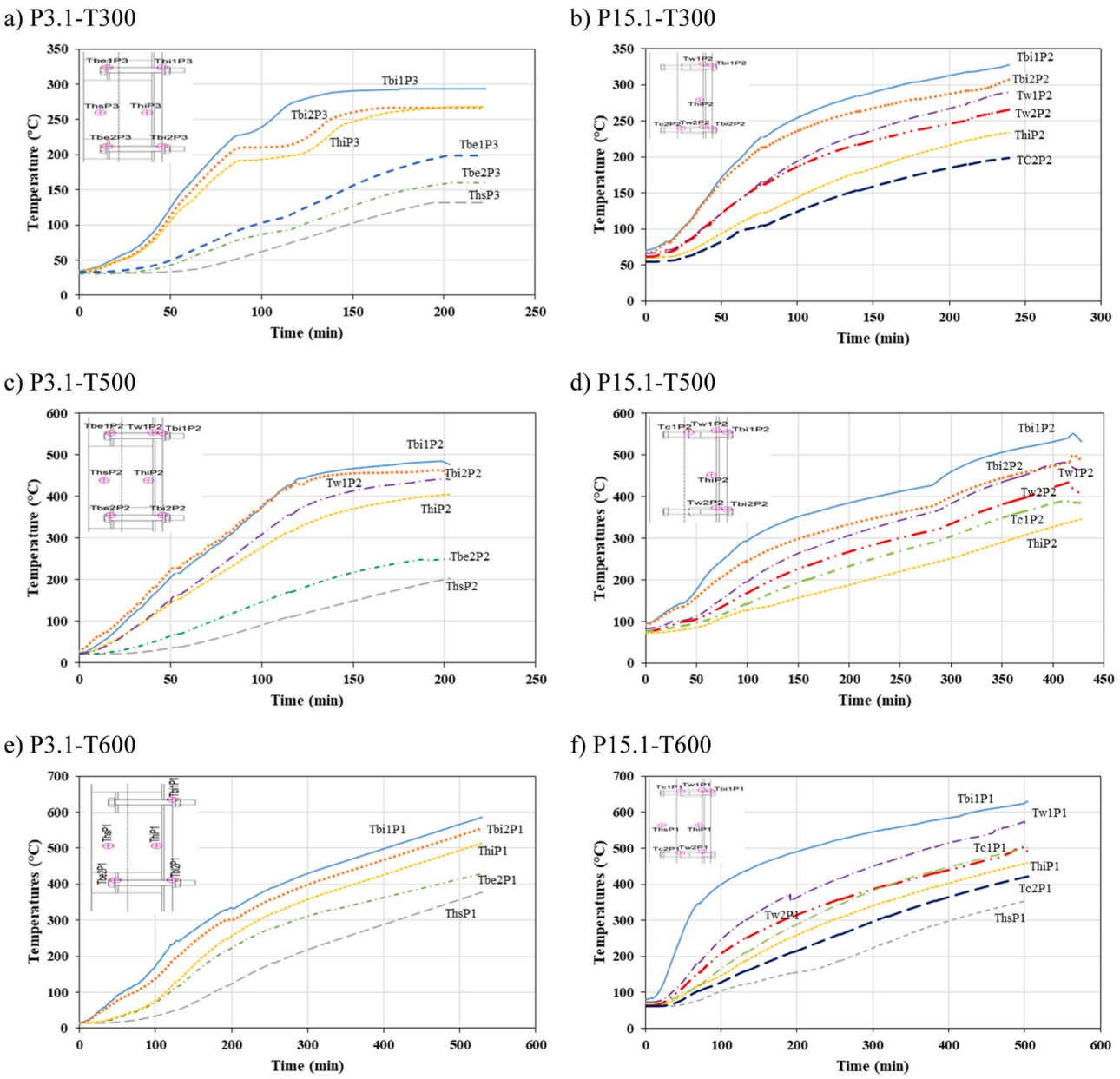

Fig. 14. Temperature evolution at the thermocouple locations for the elevated temperature tests: P3.1 (left) and P15.1 (right).

3.3. Shear response at the loading stage

The typical load-displacement curve registered during a push-out test can be divided into three stages, which are labelled in Fig. 16 for a fast identification:

1. High initial stiffness of the specimens due to friction resistance, depending on the amount of pretension force applied to the bolts (initial "vertical" segment).
2. Once the friction resistance is surpassed, a certain degree of slip in the bolt holes occurs and the stiffness of the specimen is significantly reduced (flattened stage, with smooth slope).
3. When the bolts regain contact with the inner surface of their holes, bearing and shear deformation occurs, until failure takes hold (convex part of the curve and softening branch).

Stages one and three could be easily recognized at the elevated temperature push-out tests carried out in this experimental campaign. However, the extension of the second stage was very reduced, as the hole clearance and the position of the bolts inside their holes was controlled during the installation of the specimens, so that the possible slip had a reduced impact over the mechanical response of the system.

The complete load-displacement curves captured from the performed push-out tests in this experimental work are presented hereafter, being useful for working out the degradation of the shear resistance with temperature. Fig. 17 shows the load-displacement curves registered for system 'P3.1′ (a) and 'P15.1′ (b) at the different target temperatures, where T20 stands for 20ºC, T300 stands for 300ºC, T500 stands for 500ºC and T600 stands for 600ºC. Note that the load value shown in the vertical axis is referred "per bolt", that is, the total load applied during the test divided by eight.

It should be mentioned that specimen P3.1-T500 has been marked with * in this figure, since an anomalous behaviour was encountered during the test, leading to a premature failure, as explained before. This anomaly led to an early stoppage of the test, reaching a maximum displacement of 9.56 mm, inferior to that of test P3.1-T300, and a lower

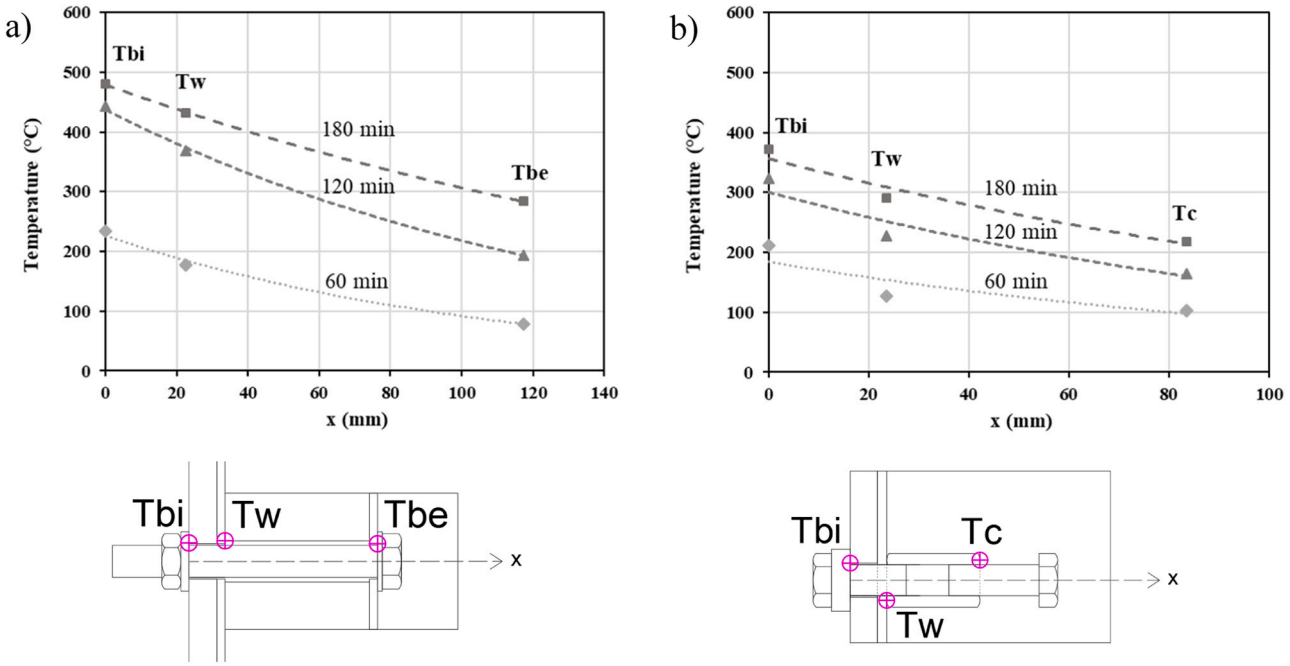

Fig. 15. Temperature gradient along the longitudinal direction of the bolt, for test P3.1-T500 (a) and P15.1-T500 (b).

Table 3
Summary of relevant temperatures obtained at the shear plane (Tbi) for all the performed push-out tests.

Test ID	Tbi1P1 (°C)	Tbi2P1 (°C)	Tbi1P2 (°C)	Tbi2P2 (°C)	Tbi1P3 (°C)	Tbi2P3 (°C)	Tbi1P4 (°C)	Tbi2P4 (°C)	Average Tbi (°C)
P3.1-T20	-	-	-	-	-	-	-	-	-
P3.1-T300	293.4	263.9	289.3	264.5	293.4	266.3	291.5	278.4	283.5
P3.1-T500	483.2	444.8	484.7	463.7	484.9	465.7	485.3	436.7	468.6
P3.1-T600	549.7	521.2	558.6	530.2	561.8	533.3	544.7	516.2	539.5
P15.1-T20	-	-	-	-	-	-	-	-	-
P15.1-T300	329.1	309.6	327.5	307.4	328.2	308.3	327.1	306.9	318
P15.1-T500	546	499.2	551.3	500.1	558.2	507.5	554.5	506.2	527.8
P15.1-T600	629.7	573.2	627.7	571.2	623.1	567.7	620.3	567.3	597.5

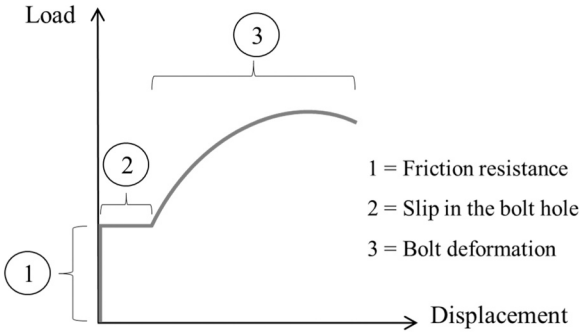

Fig. 16. Typical load-displacement behaviour observed at the push-out tests.

ultimate load than expected, therefore the values obtained for this case should not be taken as definitive.

In turn, the load-displacement curve for test P3.1-T600 shows the largest displacement of all tests (18.96 mm), given the highly ductile behaviour of the bolts observed before reaching failure.

As a reference, a comparison between the results obtained for both systems at the room temperature push-out tests carried out in this project and those previously obtained by Kozma [18] is shown in Fig. 18. It can be seen that the cylinder system results (P3.1) were quite similar, with a prediction in ultimate load, initial friction resistance and stiffness of the loading stage very close to each other, while for the coupler system (P15.1) a significant deviation was observed, with a higher friction resistance measured in the test performed in this investigation as compared with the reference test, where perhaps the initial pretension applied to the bolts was lost. In fact, both curves present the same shape, with a quantitative gap in terms of load due to the difference in the starting point at the load axis, indicating the value of the threshold load where slippage starts to occur.

The ultimate load per bolt (F_u) and maximum displacement values obtained from the two series of push-out tests performed are presented in Table 4. The higher registered ultimate load values corresponded evidently to the tests performed at ambient temperature – 148.22 kN for the cylinder system and 159.12 kN for the coupler system–, while it can be clearly seen that temperature severely affected the shear resistance of the connectors, especially above a threshold of 500 °C, with shear capacity reductions close to a 50% for both systems. The ultimate load values at a target temperature of 600 °C decreased to 69.72 kN and 51.69 kN, respectively, showing significant shear capacity reductions. By comparing the values of the two test series, it is possible to anticipate that the coupler system (P15.1) was capable to attain higher ultimate loads than the cylinder system (P3.1), although showing a lower ductility.

The main aim of the experimental push-out test series presented in this work was to investigate the degradation of the shear capacity of the studied connection systems with temperature. For that purpose, Fig. 19 shows the shear capacity loss for both test series 'P3.1′ and 'P15.1′, where the decrease in terms of maximum load per bolt along with temperature can be observed.

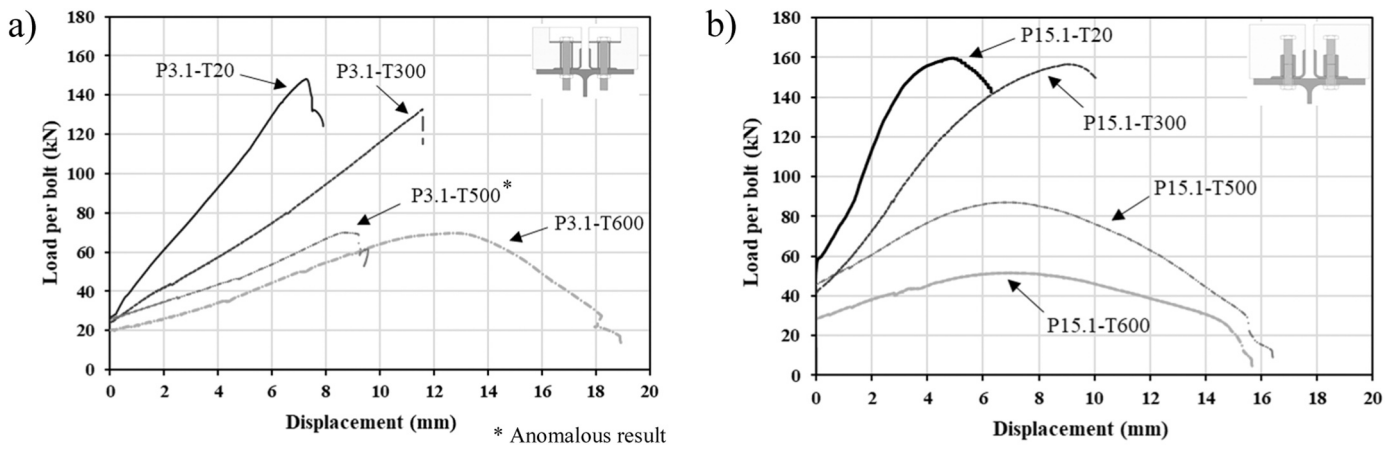

Fig. 17. Load-displacement curves at each temperature for series 'P3.1′ (a) and 'P15.1′ (b).

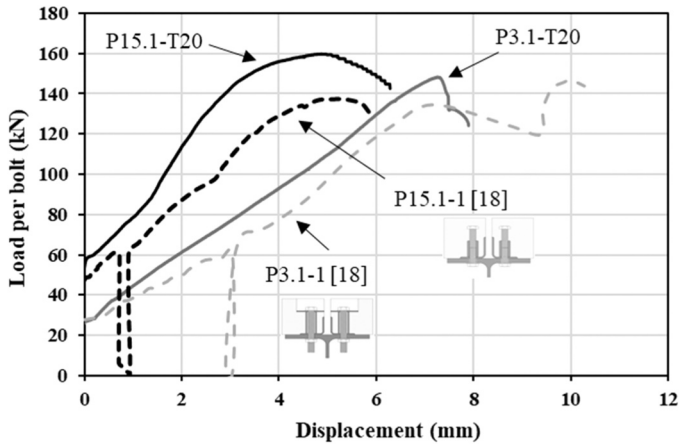

Fig. 18. Comparison between the ambient temperature push-out tests performed in this investigation and those carried out at the University of Luxembourg [18].

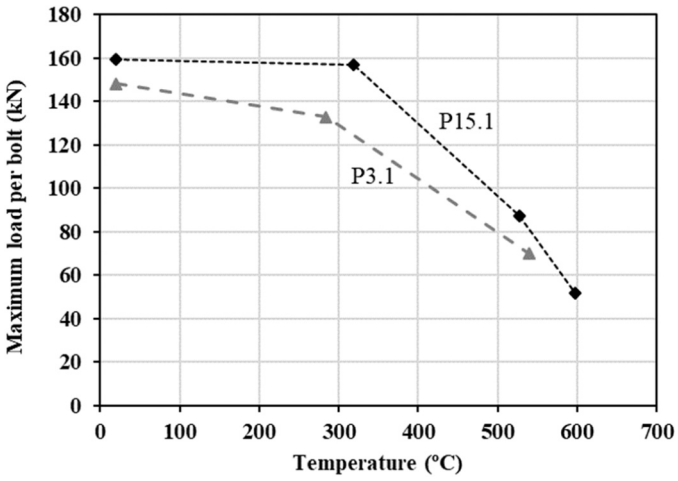

Fig. 19. Shear capacity degradation with temperature for series 'P3.1′ and 'P15.1′.

Table 4
Ultimate load values (per bolt) and maximum displacements registered at the push-out tests.

Test ID	Ultimate load F_u (kN)	Max. displacement (mm)
P3.1-T20	148.22	7.89
P3.1-T300	132.84	11.58
P3.1-T500	70.01*	9.56*
P3.1-T600	69.72	18.96
P15.1-T20	159.12	5.28
P15.1-T300	156.68	10.08
P15.1-T500	87.21	16.45
P15.1-T600	51.69	15.66

* Anomalous result

There was an obvious reduction of the shear capacity of both demountable connection systems with increasing temperatures, which caused the reduction of the yield strength of the bolts and eventually induced the shear failure at lower load values. This temperature degradation was more evident above 500ºC, where the steel yield strength was severely affected, resulting in a shear capacity reduction of about a 50% for both systems.

As it can be seen in Fig. 19, the maximum load values per bolt were higher for the coupler system (P15.1) than for the cylinder system (P3.1), in all the temperature range studied. The higher capacity values shown by the coupler system can be explained with the lower temperature development along the bolt direction that was observed and discussed in the previous temperature analysis section. It is important to note that the starting point of the maximum load at the ambient temperature tests was higher for the coupler system, therefore an improved mechanical performance at elevated temperature was also expected, which combined to the more beneficial thermal behaviour may lead to an enhanced thermo-mechanical response.

4. Analysis of results and discussion

4.1. Shear resistance of the bolts at ambient temperature

The shear resistance values obtained through the experimental testing are compared in this section with the theoretical values to assess their accuracy and how they correlate with temperature. EN 1993–1-8 [23] provides in Section 3.6.1 an expression for the calculation of the shear resistance of bolts per shear plane, see Eq. (3), which is adapted from Table 3.4 of EN 1993–1-8 for the case where the shear plane passes through the threaded portion of the bolt. The terms in this equation are α_v, with a value of 0.6 for a class of bolt 8.8, A_s which is the tensile stress area of the bolt, with a value of 245 mm^2 for an M20 bolt, and f_{ub} is the ultimate tensile strength of the bolt, with a nominal value of 800 MPa for 8.8 bolts. The real strength of the bolts was obtained from the tensile tests (see Table 1), with a measured value of the ultimate tensile strength equal to 858 MPa, which is used in the calculations instead of the

nominal value. Therefore, the expression provided in the design code has been adapted accordingly to take the measured values, thus the material safety factor γ_{M2} has been removed from this expression.

$$F_v = \alpha_v f_{ub} A \tag{3}$$

Evaluating Eq. (3), the value of the shear resistance per bolt would be $F_v = 126.13$ kN. If the experimental ultimate loads at ambient temperature (20ºC) are compared with the shear resistance per bolt obtained through this equation, then F_v accounts for a 85% of P3.1-T20 (148.22 kN) and for a 79% of P15.1-T20 (159.12 kN), therefore leading to conservative predictions.

4.2. Shear resistance of the bolts at elevated temperature

The values of the ultimate loads ($F_{u,\theta}$) registered in the elevated temperature push-out tests are presented in Table 5.

For both series, the ultimate load experiences a significant decrease as the temperature at the shear plane rises, especially when the 500ºC threshold is reached. This decrease in ultimate load is frequently associated with an increase in the displacement, which translates into a more ductile failure.

Annex D of EN1993–1-2 [26] provides expressions to calculate the fire design resistance of bolted joints under different types of loading, including shear, bearing, slip and tension. The formula utilized to calculate the fire design resistance of bolts loaded in shear at elevated temperature $F_{v,t,Rd}$ is:

$$F_{v,t,Rd} = F_{v,Rd} k_{b,\theta} \frac{\gamma_{M2}}{\gamma_{M,fi}} \tag{4}$$

where $F_{v,Rd}$ is the design shear resistance of the bolt per shear plane calculated assuming that the shear plane passes through the threads of the bolts, γ_{M2} is the partial factor at normal temperature and $\gamma_{M,fi}$ is the partial factor for fire conditions.

Strength reduction factors for bolts in shear at elevated temperature ($k_{b,\theta}$) are given in Table D.1 of the referred Annex. These reduction factors can be understood as the relationship between the elevated temperature shear resistance of the bolts to the corresponding value at ambient temperature. To compare with the experimental results, where the actual material properties are known, the formulation given in the code (Eq. 4) is modified, neglecting the partial factors of the materials, resulting in the expression shown in Eq. (5).

$$k_{b,\theta} = \frac{F_{v,t}}{F_v} \tag{5}$$

Table 5
Deduction of the experimental reduction factors for the elevated temperature push-out tests and comparison with theoretical values.

Test ID	Ultimate load $F_{u,\theta}$ (kN)	Average Tbi (°C)	Experimental reduction factor k_{b,θ_exp} ($F_{u,\theta}$ / $F_{u,20}$)	Reduction factor $k_{b,\theta}$ (Annex D EN 1993-1-2)
P3.1-T20	148.22	-	1	1
P3.1-T300	132.84	283.5	0.89	0.91
P3.1-T500	70.01*	468.6	0.47*	0.58
P3.1-T600	69.72	539.5	0.42	0.30
P15.1-T20	159.12	-	1	1
P15.1-T300	156.68	318	0.98	0.88
P15.1-T500	87.21	527.8	0.55	0.46
P15.1-T600	51.69	597.5	0.32	0.23

* Anomalous result

This section presents a comparison of the different values of the shear resistance of the bolts calculated according to Annex D of EN1993–1-2 [26] and the values obtained through the experimental push-out tests performed in this investigation.

The experimental elevated temperature reduction factors (k_{b,θ_exp}), calculated as given in Eq. (5), are shown in the fourth column of Table 5. These values have been obtained as the quotient between the ultimate load (F_u) of the corresponding elevated temperature push-out test divided by the value of the ultimate load of the test performed at 20ºC ($F_{u,20}$) for the same connection system. As it can be observed, the most significant loss of shear strength of the bolts occurs at the range of temperatures between 500 ºC and 600 ºC. As a reference for comparison, the reduction factors ($k_{b,\theta}$) taken from Table D.1 of EN 1993–1-2 [26] corresponding to the average temperature measured at the shear plane for each case are added in the last column of this table. Similar values of the reduction factors are obtained for temperatures up to 500ºC, while for 600ºC a higher deviation is obtained between the theoretical and the experimental results, with a 28% lower capacity for both P3.1 and P15.1 systems according to the strength reduction factors for bolts from Annex D, as compared to those experimentally obtained from the test results. Especially for the coupler system (P15.1) series, it can be seen how the Annex D factors result conservative in comparison with the experimental reduction factors, for all the temperatures studied.

It should be reminded that the connection type studied herein is much different from the conventional bolted connections in EN 1993–1-2. Therefore, the results obtained in this section are just an attempt to assess the applicability of the temperature reduction coefficients to other types of shear connectors, such as the demountable systems studied in this paper.

4.3. Friction resistance at the shear plane

The friction resistance at a certain shear plane can be understood as the opposition that the connection bolt offers to the applied load due to pre-tensioning before any slip can occur. It can be measured from the push-out tests results as the starting load value at the vertical axis of the load-displacement graphs. Once this threshold value is exceeded, the pre-tensioning effect at the bolt is lost and slip at the shear plane starts.

The evolution of the friction resistance with temperature ($F_{s,\theta}$), for the different push-out tests carried out, is shown in Table 6.

In views of these results, it can be stated that, for both systems, there is a progressive loss of friction resistance as the temperature rises, being more significant above the threshold of 500ºC. It can also be seen that the decrease in terms of friction resistance with temperature is more evident for the coupler system (P15.1).

The differences in friction resistance between the two systems can be

Table 6
Evolution of the friction resistance with temperature.

Test ID	Friction resistance $F_{s,\theta}$ (kN)	Pretension force $F_{p,C}$ (kN)	Friction coefficient μ_θ ($F_{s,\theta}$ / $F_{p,C}$)
P3.1-T20	26.90	142	0.19
P3.1-T300	24.16	142	0.17
P3.1-T500	25.93*	142	0.18*
P3.1-T600	20.17	142	0.14
P15.1-T20	53.73	175	0.31
P15.1-T300	41.77	175	0.24
P15.1-T500	45.80	175	0.26
P15.1-T600	28.51	175	0.16

* Anomalous result

justified with the pretension forces applied to each system, being the preloading force 33 kN higher for the coupler system (P3.1) than that for the cylinder system (P15.1). Another essential factor to take into consideration is the geometric tolerance of each system. For system P3.1, the bolt passes through a cylinder in a way that contact between the interior of this cylinder and the thread of the bolt does not occur, providing some room for the bolt to move inside the cylinder. On the contrary, the coupler utilized for system P15.1 restricts any movement of the bolt once this is screwed inside of it.

In light of the results in Table 6, it can be thought that the preloading force initially applied to the bolts may be affected by the temperature, as the friction resistance suffers a progressive reduction.

According to Section 3.9.1 in EN 1993–1-8 [23], the design slip resistance (or friction resistance) of a pre-tensioned class 8.8 bolt can be calculated by means of Eq. (6), where k_s is a factor dependent on the type of hole; n is the number of shear planes, equalling 1; μ is the slip factor at the friction plane depending on the surface treatment, which is taken as 0.3 for steel-brushed surfaces; and $F_{p,C}$ is the preloading force, equal to 142 kN for series P3.1 and 175 kN for series P15.1. Again, the material safety factor γ_{M3} has been neglected when applying the design equation, as the actual value of the preload force has been used.

$$F_s = k_s\, n\, \mu\, F_{p,C} \tag{6}$$

It should be noted that the mechanical behaviour of the demountable shear connections studied in this paper is much different from that of the conventional bolted connections. Therefore, the application of the design provisions in EN 1993–1-8 [23] for evaluating the friction resistance of the bolts is just tentative.

From Eq. (6), the experimental friction coefficient at elevated temperature (μ_θ) can be worked out as the quotient between the friction resistance obtained from the corresponding push-out tests and the preloading force, provided that the factor k_s is taken as one, which is the value corresponding to "bolts in normal holes", according to table 3.6 in EN 1993–1-8 [23]:

$$\mu_\theta = \frac{F_{s,\theta}}{F_{p,C}} \tag{7}$$

Evaluating Eq. (7), the friction coefficient values corresponding to the different temperatures tested in this experimental programme can be obtained. These values have been included in Table 6. It can be seen that the friction coefficient becomes more or less stable for the cylinder system (P3.1), with a value around 0.19 - 0.14 and a slight decrease with temperature, while for the coupler system (P15.1) this decrease is more pronounced, from a value of 0.31 at room temperature to 0.16 at 600ºC. What is also important to note is that a certain degree of slip resistance still remains at elevated temperatures, even above the threshold of 500ºC.

According to the results obtained in the push-out tests performed in this investigation, it is evident that the current hypothesis being made in Annex D of EN 1993–1-2 [26] is overly conservative, as it states that *"Slip resistant joints should be considered as having slipped in fire and the resistance of a single bolt should be determined as for bearing type bolts"*. Hence, slip resistance is not considered in the code in a fire situation. This assumption is not realistic, since it has been shown by the experimental results presented in this investigation that a certain degree of opposition to slip still exists at elevated temperatures, at least up to 600 ºC. Therefore, it is necessary to develop a formula to account for the variation of the slip resistance of the bolts at elevated temperature, which is suggested as future work.

5. Conclusions and future work

In this work, the results of a series of push-out tests have been presented to analyse the behaviour of demountable shear connectors for steel-concrete composite beams at elevated temperatures. Two different types of demountable shear connectors were studied: the so-called cylinder system and the coupler system. A total of eight push-out tests were performed, combining the mechanical load and the thermal action, applied by means of two electric heating panels. Four tests were conducted for each of the studied systems, corresponding to four different temperature levels, ranging from ambient temperature to 600 ºC.

The temperature evolution at certain relevant points of the connection system was monitored during the elevated temperature push-out tests. Also, the load-displacement curves were registered during the elevated temperature tests, showing higher ultimate loads and a higher stiffness for the coupler system, with lower ductility as compared with the cylinder system. It was found that temperature severely impacted the shear resistance of the connectors, which was evidenced by a progressive reduction in shear capacity with exposure to elevated temperatures, especially above a threshold of 500 ºC, with almost a 50% reduction of capacity for both systems. The type of failure was also affected by temperature, showing a more ductile failure with larger displacements than those measured at the ambient temperature tests. An improved thermal response was observed at the coupler system when analysing the temperature gradient along the bolts, which eventually contributed to delay its deterioration with temperature and thus enhance its mechanical performance, resulting in a higher shear capacity.

Elevated temperature reduction factors for every test series were calculated based on the push-out tests results, allowing for a comparison with those given for bolts loaded in shear in Annex D of EN 1993–1-2 [26]. Conservative results were generally obtained by applying the reduction coefficients given in the code. It was also highlighted that the hypothesis stated in Annex D – which neglects the friction resistance in the fire situation – is overly conservative, as it was proved by the experimental results presented in this work that a certain degree of friction resistance still exists at elevated temperatures.

The load-displacement curves obtained as an output from the elevated temperature push-out tests presented in this work constitute a novelty in the state-of-the-art in this field and can be very useful for their application in numerical models, as they provide a realistic representation of the mechanical behaviour of the demountable shear connectors at different temperature levels. Therefore, they can be introduced as input in the numerical models for characterizing the tangential behaviour at the steel-concrete interface and its degradation with temperature in an implicit way. This would be the next step of this investigation, where realistic numerical models for the fire behaviour of steel-concrete composite beams that make use of the studied demountable connection systems will be developed to extend the available experimental database, which will eventually serve as a basis to derive future design recommendations.

The two types of demountable shear connector systems studied in this paper proved to be adequate for reuse, since failure happened at the connector itself, while the rest of the elements of the steel-concrete composite system maintained their integrity. However, after a fire situation, the level of damage of the other components, such as the primary steel beams and the concrete slabs should be checked in order to verify their reusability.

Further research on specific fire protection measures adequate for composite floors that utilize demountable shear connections is needed to improve the reusability of these systems. Also, their residual post-fire resistance should be investigated in the future, since it plays an essential role in the reusability of the structural elements after a fire. Procedures for the correct assembly of the demountable system components should also be defined, guaranteeing the accomplishment of the structural and fire safety requirements.

Declaration of Competing Interest

The authors declare the following financial interests/personal relationships which may be considered as potential competing interests:

Manuel L. Romero reports financial support was provided by the "Conselleria d'Educació, Investigació, Cultura i Esport" of the Valencian Community (Spain) for the help provided through the project AICO/2021/297 (acronym FIREDUCE).

Acknowledgements

The authors would like to express their sincere gratitude to the "Conselleria d'Educació, Investigació, Cultura i Esport" of the Valencian Community (Spain) for the help provided through the project AICO/2021/297 (acronym FIREDUCE).

References

[1] Dallam LN. High strength bolt shear connectors - Pushout tests. Acids J 1968;65:767–9.
[2] Marshall W, Nelson H, Banerjee H. An experimental of the use of high-strength friction-grip bolts as shear connectors in composite beams. Inst Struct Eng 1971:49.
[3] Dedic DJ, Klaiber FW. High-strength bolts as shear connectors in rehabilitation work. Concr Int 1984:41–6.
[4] Sedlacek G., Hoffmeister B., Trumpf H., Kühn B., Stötzel J., Hechler O., et al. Composite bridge design for small and medium spans. Final Report. European Commission - Technical Steel Resarch, Contract No 7210-PR/0113. Luxembourg: 2003.
[5] Pavlović M. Resistance of Bolted Shear Connectors in prefabricated steel-concrete composite decks. PhD thesis. University of Belgrade; 2013.
[6] Pavlović M, Veljković M. FE validation of push-out tests: Using bolts as shear connectors. Steel Constr 2017;10:135–44. https://doi.org/10.1002/stco.201710017.
[7] Dai X, Lam D, Saveri E. Effect of concrete strength and stud collar size to shear capacity of demountable shear connectors. 04015025 J Struct Eng 2015;141. https://doi.org/10.1061/(ASCE)ST.1943-541X.0001267.
[8] Rehman N, Lam D, Dai X, Ashour AF. Experimental study on demountable shear connectors in composite slabs with profiled decking. J Constr Steel Res 2016;122:178–89. https://doi.org/10.1016/J.JCSR.2016.03.021.
[9] Wang JY, Guo JY, Jia LJ, Chen SM, Dong Y. Push-out tests of demountable headed stud shear connectors in steel-UHPC composite structures. Compos Struct 2017;170:69–79. https://doi.org/10.1016/j.compstruct.2017.03.004.
[10] Kwon G, Engelhardt MD, Klingner RE. Behavior of post-installed shear connectors under static and fatigue loading. J Constr Steel Res 2010;66:532–41. https://doi.org/10.1016/j.jcsr.2009.09.012.
[11] Chen Y-T, Zhao Y, West JS, Walbridge S. Behaviour of steel–precast composite girders with through-bolt shear connectors under static loading. J Constr Steel Res 2014;103:168–78. https://doi.org/10.1016/j.jcsr.2014.09.001.
[12] Lee S., Bradford M. Sustainable composite beams with deconstructable bolted shear connectors. Research and applications in structural engineering, mechanics and computation. 1st ed., 2013.
[13] Suwaed ASH, Karavasilis TL. Novel demountable shear connector for accelerated disassembly, repair, or replacement of precast steel-concrete composite bridges. J Bridge Eng 2017;22. https://doi.org/10.1061/(ASCE)BE.1943-5592.0001080.
[14] Feidaki E, Vasdravellis G. Horizontal push out tests on a steel-yielding demountable shear connector. Proceedings of the 12th International Conference on Advances in Steel-Concrete Composite Structures. Spain: Valencia; 2018.
[15] Ban H, Uy B, Pathirana SW, Henderson I, Mirza O, Zhu X. Time-dependent behaviour of composite beams with blind bolts under sustained loads. J Constr Steel Res 2015;112:196–207. https://doi.org/10.1016/j.jcsr.2015.05.004.
[16] Wijesiri Pathirana S, Uy B, Mirza O, Zhu X. Flexural behaviour of composite steel-concrete beams utilising blind bolt shear connectors. Eng Struct 2016;114:181–94. https://doi.org/10.1016/j.engstruct.2016.01.057.
[17] Uy B, Patel V, Li D, Aslani F. Behaviour and design of connections for demountable steel and composite structures. Structures 2017;9:1–12. https://doi.org/10.1016/j.istruc.2016.06.005.
[18] Final report REDUCE: Reuse and Demountability Using Steel Structures and the Circular Economy. Funded by the European Comission's Research Fund for Coal and Steel. 2020.
[19] Kozma A. Demountable composite beams: analytical calculation approaches for shear connections with multilinear load-slip behaviour. Doctoral thesis. PhD-FSTM-2020–29. The Faculty of Sciences, Technology and Medicine, Université du Luxembourg. 2020.
[20] Kozma A, Odenbreit C, Braun MV, Veljkovic M, Nijgh MP. Push-out tests on demountable shear connectors of steel-concrete composite structures. Structures 2019;21:45–54. https://doi.org/10.1016/j.istruc.2019.05.011.
[21] Yasuda S, Michikoshi S, Kobayashi Y, Narihara H. Experimental study on shear strength of headed stud shear connectors at high temperature. J Struct Constr Eng 2008;73:1417–23. https://doi.org/10.3130/aijs.73.1417.
[22] Chen L-Z, Ranzi G, Jiang S-C, Tahmasebinia F, Li G-Q. Performance and design of shear connectors in composite beams with parallel profiled sheeting at elevated temperatures. Int J Steel Struct 2016;16:217–29. https://doi.org/10.1007/s13296-016-3016-x.
[23] CEN. EN 1993–1-8. Eurocode 3: Design of steel structures - Part 1–8: Design of joints 2005.
[24] CEN. EN 1994–1-1, Eurocode 4: Design of composite steel and concrete structures. Part 1.1: General rules and rules for buildings 2004.
[25] European Commission. Directorate General for Research and Innovation. Development of improved shear connection rules in composite beams (DISCCO), Final Report, Project No. RFCS-CT-2012–00030. Brussels, Belgium: 2017.
[26] CEN. EN 1993–1-2, Eurocode 3: Design of steel structures, Part 1.2: General rules – Structural fire design 2005.